Superclimbing dislocation with a Coulomb-type interaction between jogs

Longxiang Liu*
Department of Modern Physics, University of Science and Technology of China, Hefei, Anhui 230026, China and Department of Engineering & Physics and the Graduate Center, CUNY, Staten Island, New York 10314, USA

Anatoly B. Kuklov
Department of Engineering & Physics and the Graduate Center, CUNY, Staten Island, New York 10314, USA

(Received 14 January 2018; published 23 March 2018)

The main candidate for the superfluid pathways in solid ^{4}He are dislocations with Burgers vector along the *hcp* symmetry axis. Here we focus on the quantum behavior of a generic edge dislocation which can perform superclimb; that is, it can climb due to the superflow along its core. The role of the long-range elastic interactions between jogs is addressed by Monte Carlo simulations. It is found that such interactions do not change qualitatively the phase diagram found without accounting for the long-range forces. Their main effect consists of renormalizing the effective scale determining the compressibility of the dislocation in the Tomonaga-Luttinger liquid phase. It is also found that the quantum rough phase of the dislocation can be well described within the Gaussian approximation which features off-diagonal long-range order (ODLRO) in one dimension for the superfluid order parameter along the core.

DOI: 10.1103/PhysRevB.97.104510

I. INTRODUCTION

Dislocations are linear topological defects in crystals. These objects determine the amazing variety of properties of real materials (see in Ref. [1]). In most cases dislocations are described as classical strings producing long-range strain and stress around their cores. This stress is responsible for interactions between dislocations and, correspondingly, for the emerging collective structures and the strongly nonlinear dynamics—classical plasticity. A complete description of dislocation ensembles remains a tantalizing technological problem which is also of fundamental importance.

The role of quantum mechanics in dislocation dynamics has also been discussed. Generating kink-antikink pairs along dislocation by quantum tunneling under stress has been described in Ref. [2]. However, beyond this result the role of quantum mechanics in dislocation induced plasticity in technological materials remains largely an open question. In metals, edge dislocation has been proposed to induce superconductivity by strain within some radius from its core [3]. This model is based on a phenomenological form of the minimal interaction between isotropic strain and a scalar superconducting order parameter. The experimental observation consistent with the proposal has been reported in Ref. [4]. It is worth mentioning that the main role of the dislocations in this effect is to create a strain which lowers locally the temperature of the superconducting transition, with the dislocation dynamics remaining irrelevant.

Simulations of screw dislocation along the C_6 symmetry axis in solid ^{4}He have revealed that its core can be superfluid at low temperature and pressures close to the melting line [5]. Symmetry of the problem indicates that the interaction between the strain field and superfluid order parameter must be of second order with respect to the strain [6]. A significant difference with the situation in superconductors is that in solid ^{4}He the same particles form crystalline order (modified by the dislocation topology) and participate in forming algebraic off-diagonal correlations. In this sense a crystal containing such a dislocation represents an example of a supersolid phase of matter. The experimental observation [7] of the supercritical flow through the solid ^{4}He is consistent with the simulations [5]—at least at the qualitative level.

The most dramatic effect where quantum mechanics impacts dislocation dynamics has been observed in simulations of the edge dislocation with Burgers vector along the C_6 axis [8]. The dislocation dynamics turned out to be strongly intertwined with the superfluidity along the dislocation core which results in the so-called superclimb effect: the dislocation climb supported by the superflow along the core. This effect is essentially a mechanism for injecting ^{4}He atoms into the solid from a superfluid with the help of the Vycor "electrodes"—in line with the experimental observation of the so-called syringe effect [9]. According to the superclimb mechanism one dislocation climbing across a sample can build or remove one layer of atoms.

As discussed in Ref. [8] within the Gaussian approximation, a generic superclimbing dislocation (that is, tilted in the Peierls potential) is characterized by an excitation spectrum which is parabolic in the momentum along the core. Thus, such a dislocation represents an example of a non-Luttinger liquid [10]. However, recent analysis [11] of a generic superclimbing dislocation beyond the Gaussian approach has found that quantum fluctuations can restore the Tomonaga-Luttinger liquid (TLL) behavior of the dislocation. This effect implies that a superclimb of the dislocation is suppressed in

*llx1991@mail.ustc.edu.cn

the limit of zero temperature. In other words, the dislocation undergoes a transition or crossover from a thermally rough to a quantum smooth state. Furthermore, the phase diagram of the dislocation in the plane of the crystal shear modulus G and the superfluid stiffness ρ_s along the core features a line of the quantum phase transition between TLL and insulator, where the superflow along the core becomes impossible.

The analysis [11] was based on the string model of dislocation coupled to the superfluid phase [8] which ignores long-range elastic forces between dislocation shape fluctuations. At this juncture it is important to emphasize the crucial role the long-range forces play in the quantum glide of a dislocation [12]. It was found that an arbitrary small long-range interaction between kinks of the dislocation aligned with Peierls potential suppresses the quantum roughening transition. This transition is essentially the same as occurs in a TLL confined in a lattice with integer filling. The analogy with superclimbing dislocation, which also undergoes such a transition [11], raises the question of whether long-range forces between jogs should also eliminate the transition and produce an insulating phase of the superclimbing dislocation.

In this paper we analyze a superclimbing dislocation with long-range forces between jogs. Our main result is that, in a sharp contrast with the gliding dislocation [12], all the features observed in Ref. [11] for superclimbing dislocation remain qualitatively unaltered by the long-range forces. The role of the long-range forces is reduced to the renormalization of the dislocation compressibility as a function of the shear modulus and strength of the long-range forces into a single master curve featuring a scaling-type dependence.

II. LINEARIZED ANALYSIS OF THE SUPERCLIMB WITH COULOMB-TYPE INTERACTION

A. Dislocation action

A superclimbing dislocation with its core along the x direction and Burgers vector along the z direction can be modeled as an elastic string of length L which can climb in the y direction along the XY plane. The climb is supported by superflow along the core [8]. Similar to the work in Ref. [11], we consider dislocation with a finite density of jogs of one sign, that is, a dislocation which is tilted with respect to the Peierls potential rendering this potential essentially irrelevant [10,11]. The corresponding action in imaginary time

$$S = S_0[\phi, y] + S_{\rm int}[y] \tag{1}$$

is a functional of two variables: $y = y(x,\tau)$ describing the position of the dislocation in the XY plane and imaginary time τ, and the superfluid phase $\phi = \phi(x,\tau)$ defined along the core. Here

$$S_0[\phi, y] = \int_0^\beta d\tau \int_0^L dx \Big[-i(y + n_0)\partial_\tau \phi + \frac{\rho_0}{2}(\partial_x \phi)^2 + \frac{\kappa_0}{2}(\partial_\tau \phi)^2 + \frac{G_1}{2}(\partial_x y)^2 - \mu y \Big], \tag{2}$$

(in units $\hbar = 1$, $K_B = 1$) stands for the short-range part of the action considered in Ref. [11] with $\beta = 1/T$, and

$$S_{\rm int}[y] = \frac{G_2}{2} \int_0^\beta d\tau \int_0^L dx \int_0^L dx' \frac{\partial_x y \partial_{x'} y}{|x - x'| + a}, \tag{3}$$

describes the long-range interaction between jogs, with a being a short-range cutoff (of the order of interatomic distance). This interaction is induced by exchanging bulk phonons between parts of the string separated by a distance $x - x'$ [13,14]. The other notation used in Eqs. (2) and (3) is as follows: ρ_0 and κ_0 are superfluid stiffness and compressibility, respectively; n_0 stands for the average filling factor; the parameters $G_{1,2}$ are determined by crystal shear modulus and symmetry (we consider the isotropic approximation); and μ is the external bias by chemical potential counted from the value at which the dislocation is in its equilibrium position $y = 0$.

We impose the boundary condition $y(0,\tau) = y(L,\tau) = 0$ in order to avoid the zero mode which corresponds to the uniform shift of the string (costing no energy). Since we are considering the limits of low (Matsubara) frequencies $\omega \to 0$ and large wavelengths $q \to 0$, we omit the kinetic energy term $\sim(\partial_\tau y)^2$ of the dislocation climb. The main contribution to the kinetic energy comes from the superflow along the dislocation core (X direction).

Full statistical description of the dislocation implies evaluation of the partition function

$$Z = \int \mathscr{D}\phi\, \mathscr{D}y\, \exp(-S) \tag{4}$$

as the functional integral over ϕ and y, where the compact nature of the phase ϕ (that is, the possibility of existence of instantons) must be taken into account.

B. Gaussian approximation

The action (1) can be analyzed in a Gaussian approximation by ignoring the compact nature of the phase ϕ (and, thus, treating it as a Gaussian variable). Then, it is straightforward to obtain the spectrum of the excitations from the variational equations of motion $\delta S/\delta y = 0$, $\delta S/\delta \phi = 0$:

$$-i\partial_\tau \phi - G_1 \partial_x^2 y - G_2 \partial_x \int dx' \frac{\partial_{x'} y}{|x - x'| + a} = \mu, \tag{5}$$

$$i\partial_\tau y - \rho_0 \partial_x^2 \phi - \kappa_0 \partial_\tau^2 \phi = 0. \tag{6}$$

Since we are interested in the low energy limit, the last term in Eq. (6) can be dropped. Then, we arrive at

$$\partial_\tau^2 \phi - G_1 \rho_0 \partial_x^4 \phi - G_2 \rho_0 \partial_x \int dx' \frac{\partial_{x'}^3 \phi}{|x - x'| + a} = 0. \tag{7}$$

As discussed in Refs. [8,11] for $G_2 = 0$ this corresponds to the parabolic spectrum $\omega = \sqrt{G_1 \rho_0} q^2$ with respect to the momentum q along the core, where ω corresponds to frequency in real time. At finite G_2 this spectrum acquires the logarithmic correction $\omega = \sqrt{\rho_0 (G_1 + G_2 \gamma \ln[1 + 1/(qa)^2]}\, q^2$, where the Fourier transform of the long-range kernel $1/[|x - x'| + a]$ is taken as $\approx \gamma \ln[1 + 1/(qa)^2]$ with $\gamma \sim 1$.

Equation (7) should be compared with the standard TLL equation of motion

$$\kappa_0 \partial_\tau^2 \phi - \rho_0 \partial_x^2 \phi = 0, \tag{8}$$

following from the action (2) in the absence of the Berry term ($\sim i y \partial_\tau \phi$). The corresponding spectrum (in real time) $\omega = \sqrt{\rho_0/\kappa_0}\, q$ is linear in q.

The parabolic spectrum of superclimbing dislocation can be interpreted in terms of the diverging compressibility κ—the *giant isochoric compressibility* [8]. It determines how much matter can be supplied to (or removed from) the sample due to the dislocation superclimb induced by a variation of chemical potential μ. In the Gaussian approximation $\kappa = T\partial^2 S/\partial\mu^2$, where ϕ and y are solutions of the equations of motion in the limit $\omega \to 0$ and μ is set to zero after the differentiation. The response can be also found for μ being nonuniform. Then, in Fourier $\kappa^{-1} = \{G_1 + G_2\gamma \ln[1 + 1/(qa)^2]\}\, q^2$, which leads to the divergence in the limit $q \to 0$. In particular, for the longest wavelength $q \approx 1/L$

$$\kappa \approx \frac{L^2}{G_1 + G_2\gamma \ln[1 + (L/a)^2]}, \tag{9}$$

or $\kappa \sim L^2/[G_2 \ln(L/a)]$ as $L \to \infty$.

It is important to emphasize that the divergence (9) does *not* imply that a three-dimensional (3D) sample permeated by a network of such dislocations should show a diverging 3D compressibility. As discussed in Refs. [11,15] for $G_2 = 0$, the diverging κ for one dislocation means that a sample of solid ^{4}He permeated by a uniform network of superclimbing dislocations exhibits the 3D response on chemical potential which is *independent* of the dislocation density. In other words, the 3D isochoric compressibility (response on chemical potential) of the solid becomes comparable to that of a liquid. This property is the basis for the syringe effect [8,9]—injecting (withdrawing) matter uniformly into (from) a solid from one point of a contact with the network.

We note that at finite G_2, that is, when the long-range forces of Eq. (3) are included, the response becomes suppressed logarithmically with respect to a typical length L of superclimbing segments. Indeed, a typical element of the network of volume $\sim L^3$ can acquire (or lose) $\sim yL$ extra particles due to the bias $\mu \neq 0$. The value of y in the quasistatic limit follows from Eq. (5) as $y \sim \mu L^2/(G_2 \ln L)$. Thus, the fractional mass change becomes logarithmically suppressed as $\approx yL/L^3 \sim \mu/(G_2 \ln L)$ in the limit $L \to \infty$ of low density $L^{-2} \to 0$ of the superclimbing dislocations.

C. ODLRO of superclimbing dislocation at $T = 0$

It is interesting to note that, counterintuitively, in the superclimbing regime the dislocation is characterized by off-diagonal long-range order (ODLRO) *not* expected in one dimension (1D) at $T = 0$. To demonstrate this, the density matrix $\langle\psi^*(x,\tau)\psi(x',\tau)\rangle$ of the field $\psi = \exp(i\phi)$ can be calculated within the Gaussian approximation, Eqs. (1)–(4). Ignoring the log corrections we find

$$\langle\psi^*(x,\tau)\psi(x',\tau)\rangle = \exp\left(-\frac{\sqrt{G_1}}{2\pi a\sqrt{\rho_s}}\right) \tag{10}$$

in the limit $|x - x'| \to \infty$, where the coordinates x, x' are along the core and $1/a$ stands for the upper cutoff of the momentum integration.

The emergence of the ODLRO in 1D is unexpected. As it is clear from above, it is a direct consequence of the parabolic excitation spectrum of the dislocation. As discussed in Ref. [11] and will be addressed further below, this spectrum undergoes a transformation into the linear dispersion in the quantum limit giving rise to the TLL phase—as long as the external bias μ is below some threshold. In this phase the density matrix demonstrates the standard algebraic order $\langle\psi^*(x,\tau)\psi(x',\tau)\rangle \sim 1/|x - x'|^c$, with the exponent determined by the emerging Luttinger parameter $K_{\rm eff} = \sqrt{\rho_0\kappa_{\rm eff}}$ as $c = 1/(2\pi K_{\rm eff})$. (The value of the effective compressibility $\kappa_{\rm eff}$ will be discussed below.) However, as shown in Ref. [11] and will also be discussed below, the bias μ can destroy the TLL phase by inducing the quantum rough phase of the dislocation, that is, the phase characterized by the superclimb. Accordingly, the ODLRO is reinstated at $T = 0$.

It should also be mentioned that, in contrast to 3D, this ODLRO is fragile: at any finite temperature T the density matrix becomes exponentially decaying as

$$\langle\psi^*(x,\tau)\psi(x',\tau)\rangle = \exp\left(-\frac{T|x - x'|}{2\pi\rho_0}\right), \tag{11}$$

in the limit $|x - x'| \geqslant \sqrt{\sqrt{G_1\rho_0}/T}$.

As discussed in Ref. [11], the linearized analysis of the system does not describe the effect of emergence of the TLL and the insulating behavior as $T \to 0$ and $L \to \infty$. The compact nature of the superfluid phase needs to be taken into account. This can be done in the dual representation as explained in the following sections.

III. DUAL DESCRIPTION

To go beyond the Gaussian approximation by allowing instantons, we discretize space-time into sites (x,τ) on a square lattice, and take into account compact nature of the phase ϕ. This implies transforming the integration $\int d\tau \int dx \ldots$ into the summation $\sum_\tau \sum_x \Delta\tau\Delta x \ldots$ over the space-time lattice. Specially, we set $\Delta x = a$ and select a as the unit of length naturally determined by a typical interatomic distance. The imaginary time increment $\Delta\tau = \beta/N_\tau$ is determined by the number of time slices N_τ. Correspondingly, the continuous derivatives $\partial_x\phi(x,\tau)$, $\partial_\tau\phi(x,\tau)$, and $\partial_x y$ transform to $\nabla_x\phi(x,\tau) \equiv \phi(x + 1,\tau) - \phi(x,\tau)$, $\partial_\tau\phi \to \nabla_\tau\phi(x,\tau)/\Delta\tau$, with $\nabla_\tau\phi \equiv \phi(x,\tau + \Delta\tau) - \phi(x,\tau)$ and $\nabla_x y \equiv y(x + 1,\tau) - y(x,\tau)$. Then, the action (1)–(3) becomes

$$\begin{aligned} S(\phi,y) = \sum_{(x,\tau)}\Bigg[& -i(y + n_0)\nabla_\tau\phi + \frac{\Delta\tau\rho_0}{2}(\nabla_x\phi)^2 \\ & + \frac{\kappa_0}{2\Delta\tau}(\nabla_\tau\phi)^2 + \frac{\Delta\tau G_1}{2}(\nabla_x y)^2 \\ & + \frac{\Delta\tau G_2}{2}\sum_{x'}\frac{\nabla_x y\nabla_{x'} y}{|x - x'| + 1} - \Delta\tau\mu y\Bigg]. \end{aligned} \tag{12}$$

Formally speaking, the limit $N_\tau \to \infty$ at fixed β should be approached.

Compactness of ϕ can be taken into account within the Villain approximation [16] $\vec{\nabla}\phi \to \vec{\nabla}\phi + 2\pi\vec{m}$ with $\vec{m}$ being integer vector variables defined on bonds between neighboring sites. Then, ϕ can be regarded as a noncompact Gaussian

variable. Thus, the action (12) becomes

$$S(\phi,y,m_x,m_\tau) = \sum_{(x,\tau)}\Bigg[-i(y+n_0)(\nabla_\tau\phi+2\pi m_\tau) + \frac{\Delta\tau\rho_0}{2}(\nabla_x\phi+2\pi m_x)^2+\frac{\kappa_0}{2\Delta\tau}(\nabla_\tau\phi+2\pi m_\tau)^2 + \sum_{x'}\frac{\Delta\tau(G_1\delta_{x,x'}+G_2)}{2}\frac{\nabla_x y\nabla_{x'}y}{|x-x'|+1}-\Delta\tau\mu y\Bigg]. \tag{13}$$

Accordingly, the partition function includes summation over the bond integers:

$$Z=\sum_{m_x,m_\tau}\int\mathscr{D}y\int\mathscr{D}\phi\ e^{-S(\phi,y,m_x,m_\tau)}. \tag{14}$$

The Poisson identity $\sum_m f(m)\equiv\sum_J\int dm f(m)e^{2\pi imJ}$ allows tracing out all m_x and m_τ at each bond between neighboring sites and also explicitly integrating out the ϕ,y variables. Furthermore, similar to the approach in Ref. [11], we focus on the long-wave limit by retaining only the lowest order of spatial derivatives. Then, the partition function, Eqs. (14) and (13), finally becomes

$$Z=\sum_{\{J_x\}}\sum_{\{J_\tau\}}e^{-S_J} \tag{15}$$

(up to a constant factor), where $J_x=J_x(x,\tau)$ stands for the integer current oriented from the site (x,τ) along the X bond toward the site $(x+1,\tau)$; similarly, $J_\tau=J_\tau(x,\tau)$ is an integer current along the time bond between the sites (x,τ) and $(x,\tau+\Delta\tau)$; both J_x and J_τ can be positive or negative; and

$$S_J=\sum_{(x,\tau)}\Bigg[\frac{1}{2\widetilde{\rho}_0}(J_x)^2-\widetilde{\mu}J_\tau + \frac{1}{2}\sum_{x'}(\widetilde{G}_1\delta_{x,x'}+\widetilde{G}_2)\frac{\nabla_x J_\tau\nabla_{x'}J_\tau}{|x-x'|+1}\Bigg], \tag{16}$$

where $\widetilde{G}_1=G_1\Delta\tau$, $\widetilde{G}_2=G_2\Delta\tau$, $\widetilde{\mu}=\mu\Delta\tau$, and $\widetilde{\rho}_0=1/[2\ln(2/\rho_0\Delta\tau)]$ (in the limit $\Delta\tau\to 0$) [16].

As discussed in Ref. [11], the qualitative structure of the results does not change in the limit $\Delta\tau\to 0$. Thus, in order to understand the main features it is sufficient to consider $\Delta\tau$ fixed as, say, $\Delta\tau=1$.

The integration of the ϕ variable results in the local constraint which is Kirchhoff's current conservation rule. It can be represented as

$$\vec{\nabla}\cdot\vec{J}=0, \tag{17}$$

where the discrete divergence is defined as $\vec{\nabla}\cdot\vec{J}=J_x(x+1,\tau)-J_x(x,\tau)+J_\tau(x,\tau+1)-J_\tau(x,\tau)$. This means that the physical configuration space contributing to Z consists of closed loops of the J currents—exactly akin to the J-current model introduced in Ref. [17]. We emphasize that the model in Eqs. (15)–(17) represents a dual version of the original model of Eqs. (1)–(4), where the original continuous variables are replaced by the discrete bond currents J_x, J_τ, and the constraint (17).

Linear response

The linear response of the system is described in terms of the renormalized superfluid stiffness [18]

$$\rho_s=\frac{L}{\beta}\langle W_x^2\rangle,\quad W_x=\frac{1}{L}\sum_{(x,\tau)}J_x(x,\tau), \tag{18}$$

and the renormalized compressibility

$$\kappa=-\frac{\beta}{L}\frac{\partial^2\ln Z}{\partial\mu^2}=\frac{\beta}{L}\left[\langle W_\tau^2\rangle-\langle W_\tau\rangle^2\right]. \tag{19}$$

The quantities W_x, $W_\tau=N_\tau^{-1}\sum_{(x,\tau)}J_\tau(x,\tau)$ are integers and have the geometrical meaning of windings of the lines formed by the J currents. By the construction, W_τ is also the total particle number N in the system. The winding numbers are topological characteristics of a particular configuration and their values cannot be changed by continuous deformation of the loops.

Simulations have been performed by the worm algorithm [19]. It is also convenient to introduce the quantity

$$\kappa_1=\frac{\langle N\rangle}{L\mu}=\frac{\langle W_\tau\rangle}{L\mu}. \tag{20}$$

Both κ and κ_1 coincide with each other as $\mu\to 0$. In general, κ,κ_1 are related by the exact formula $\kappa=d(\mu\kappa_1)/d\mu$. Despite that, statistical errors of simulations can be quite different for both quantities.

IV. PHASES OF SUPERCLIMBING DISLOCATION

The action (16) has been studied in Ref. [11] in the absence of the long-range term, that is, for the case $\widetilde{G}_2=0$. The main result of this study is that as L and β both increase, the non-TLL phase crosses over to either TLL or insulator regardless of the filling factor. The line of Berezinskii-Kosterlitz-Thouless (BKT) transitions separates both phases in the plane (ρ_0,G_1) [11] for $\mu=0$.

As discussed in Ref. [11], the BKT transition should not occur in this system according to the elementary analysis based on counting the scaling dimensions. The "paradox" could be resolved if the discrete nature of the variables J_x, J_τ is taken into account [20]: as ρ_0^{-1} or G_1 increases, the discrete gradient term $\sim(\nabla_x J_\tau)^2$ in Eq. (16) becomes effectively $\sim J_\tau^2$. This implies the standard XY model behavior corresponding to integer filling. Accordingly, the BKT transition should be expected. In this context, then, it is worth recalling the result [12] where it was shown that the long-range forces suppress quantum roughening of gliding dislocation aligned with Peierls potential. Such a dislocation is formally described by the XY model (despite that there is no superfluid core), and the suppression of the roughening is interpreted as the insulating state of the effective Luttinger liquid of kinks. Furthermore, the insulating state of kinks has been shown to emerge at an arbitrary small value of the long-range interaction. In other words, the long-range interaction eliminates the BKT transition in this system [12].

Thus, the question arises if the same forces in action (16) should suppress the superfluidity along the core of the superclimbing dislocation—also at an arbitrary small value of G_2. Clearly, if $\nabla_x J_\tau$ is replaced by $\sim J_\tau$ in action (16) one

would arrive at exactly the same action studied in Ref. [12]. Then, the answer would be positive to the above question.

As will be shown below, our numerical results for model (16) contradict this logic. More specifically, we find that there is a separatrix in the finite scaling behavior which occurs at finite values of G_2 of the order of unity. This separatrix indicates the boundary between TLL and the insulator. Furthermore, we show that the effect of finite G_2 in Eq. (16) is reduced to renormalization of G_1, so the phase diagram constructed in Ref. [11] for the case $G_2 = 0$ can be simply redrawn in terms of the renormalized G_1.

Renormalized compressibility in the quantum limit

The compressibilities in Eqs. (19) and (20) show "giant" values $\sim L^2$ at finite β as $L \to \infty$ [11]. This feature is intimately connected with the superclimb effect and the parabolic excitation spectrum [8]. However, simulations of the full model in the limit $\beta \sim L \to \infty$ for $G_2 = 0$ have found that the compressibility becomes finite if G_1 does not exceed some critical value G_c for a given ρ_0. If $G_1 > G_c$, the compressibility vanishes, which is a signal of the insulating behavior.

The results of Monte Carlo (MC) simulations performed for finite G_2 are shown in Fig. 1. It depicts compressibility κ at various L, with $\beta = L$, and various values of G_1 for $G_2 = 1.0$, $\rho_0 = 4$, and $\mu = 0$. As can be seen, κ asymptotically approaches finite values $\kappa_{\rm eff}$ in the limit $L = \infty$, if G_1 is below some critical value which can be estimated as $G_c \approx 2.1$. This behavior is qualitatively the same as observed in Ref. [11] for $G_2 = 0$. If G_1 exceeds G_c, the compressibility flows to zero as can be clearly seen in Fig. 1. This feature, indicating the quantum transition toward the insulator, is also qualitatively the same as observed in Ref. [11] for $G_2 = 0$. Here we did not study in detail whether the transition remains in the BKT universality. Instead, we will give a strong argument in favor of the BKT universality in the presence of long-range forces, that is, at finite G_2.

The behavior of κ vs L for $G_1 = 1.5$ and varying G_2 is shown in Fig. 2. This plot also shows the saturation to finite values $\kappa = \kappa_{\rm eff}$, if G_2 is below some critical value, $G_{2c} \approx 2.1$,

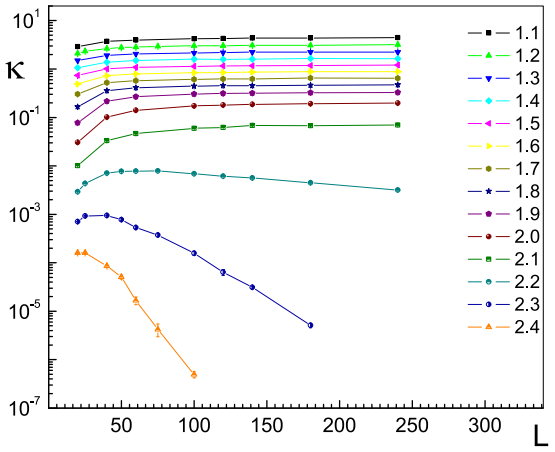

FIG. 1. Compressibility κ vs $L = 1/T$ for various values of G_1 shown in the legend at $G_2 = 1.0$ and $\rho_0 = 4$, $\mu = 0$.

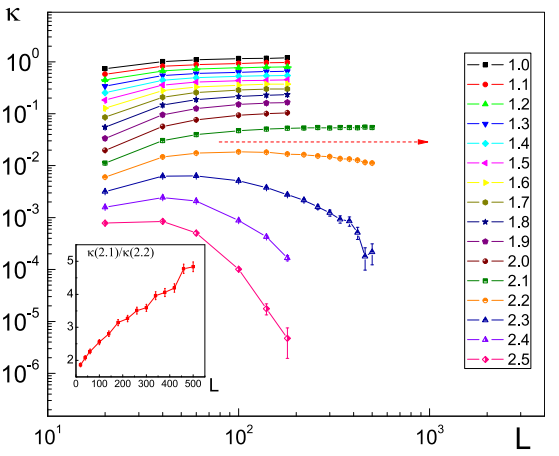

FIG. 2. Compressibility κ vs $L = 1/T$ for various values of G_2 shown in the legend at $G_1 = 1.5$ and $\rho_0 = 4$, $\mu = 0$. The dashed line indicates the approximate position of the separatrix. Insert: the ratio $\kappa(G_1 = 1.5, G_2 = 2.1)/\kappa(G_1 = 1.5, G_2 = 2.2)$ indicating different types of behavior above and below the separatrix.

and the flow toward the insulator at $G_2 > G_{2c}$. To emphasize the separatrix type of feature (marked by the dashed line in Fig. 2), that is, separating the TLL and the insulating phases, the ratio of $\kappa(G_2 = 2.1)$, which shows no visible dependence on L over the extended range, to $\kappa(G_2 = 2.2)$, which shows deviations from the asymptotic saturation, is presented in the inset to Fig. 2. A strong divergence of the ratio with growing L emphasizes the separatrix.

The asymptotic values $\kappa_{\rm eff}$ vs G_1, G_2 are presented in Fig. 3 for various combinations of the arguments. (The "asymptotic" values of κ from the curves in Figs. 1 and 2 showing no asymptotic behavior were read off from the largest size simulated.) These curves appear to be unrelated to each other. However, it is important to note that all the data from Fig. 3 can be collapsed onto a single master curve $\kappa_{\rm eff}$ vs the variable

$$G_{1R}(G_1, G_2) = G_1 + A\frac{G_2^{0.686}}{1 + 0.2G_1}, \tag{21}$$

where $A = 0.93 \pm 0.05$, which can be viewed as G_1 renormalized in the presence of the long-range interactions. This

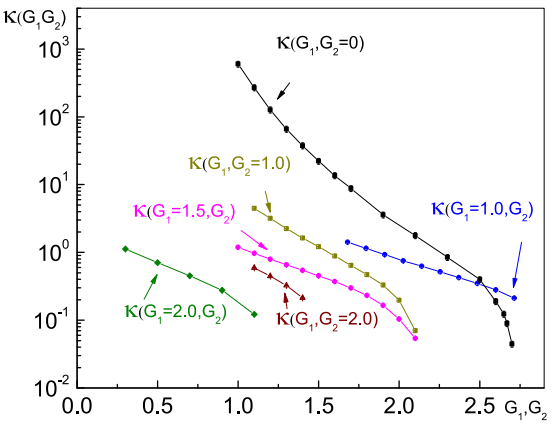

FIG. 3. Asymptotic values $\kappa_{\rm eff}$ of κ for various values of G_1 and $G_2 = 1.0$. The data for $G_2 = 0$ are taken from Ref. [11].

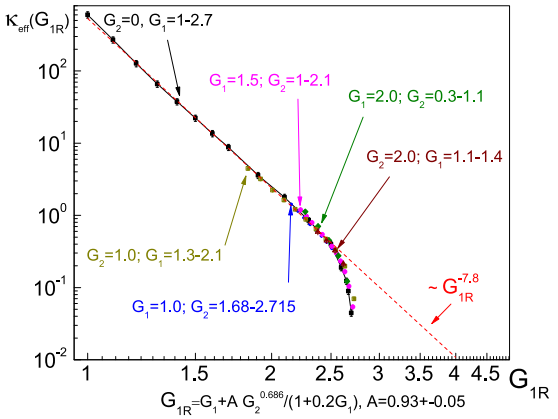

FIG. 4. Master curve $\kappa_{\rm eff}$ taken from Fig. 3 and replotted vs G_{1R}. The parameter A has been adjusted for some sets to better fit the master curve within 5% of deviations, while other parameters were kept fixed for all sets.

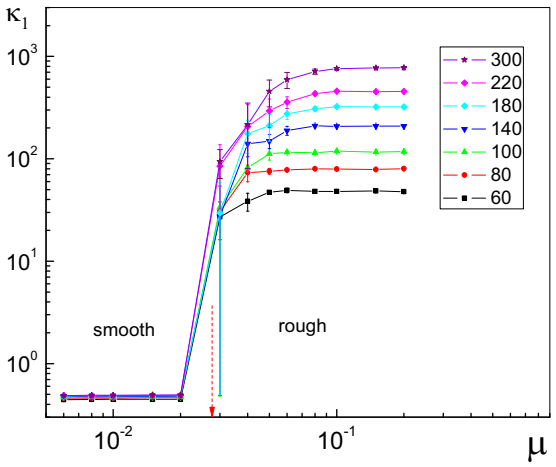

FIG. 5. κ_1 vs μ for various L up to $L = 300$ with $G_1 = 1.5$, $G_2 = 1.5$, $\rho_0 = 4$, $T = 0.05$.

interpretation is justified because all the data at finite G_2 can be collapsed to the curve κ vs G_1 at $G_2 = 0$ (from Ref. [11]). The resulting dependence is shown in Fig. 4. The master curve indicates that all the data $\kappa_{\rm eff}(G_1,G_2)$ satisfy the relation $\kappa_{\rm eff}(G_1,G_2) = \kappa_{\rm eff}(G_{1R},0)$ (within the error of 5%) over its whole range spanning TLL and insulator. Thus, we conclude that as long as G_{1R} is below its critical value G_c (which is $G_c \approx 2.7$ for $\rho_0 = 4$) there is a finite domain of G_2 within which the TLL behavior persists. This domain corresponds to the dotted line $\sim G_{1R}^{-7.8}$ in Fig. 4, with the deviations indicating the flow toward the insulating phase. Thus, the long-range interactions do not change qualitatively the nature of the phase diagram found in Ref. [11]. Its main role is in renormalizing G_1 to G_{1R}, Eq. (21).

V. IMPACT OF LONG-RANGE FORCES ON SUPERCLIMB INDUCED BY BIAS

The emergence of TLL behavior and the corresponding suppression of the superclimb can be viewed from a different perspective. The giant compressibility [8,11] becomes possible because the dislocation can climb, thanks to the supercurrents along the core supplying the matter needed to support this nonconservative motion of the core. This determines the rough phase of the dislocation, when the mean-square displacement of the core position exhibits fluctuations logarithmically diverging as $L \to \infty$. As shown in Ref. [11] and discussed above, at zero bias by chemical potential, μ, such fluctuations become suppressed in the quantum limit so that the TLL behavior emerges. In other words, the rough phase of the superclimbing dislocation at zero bias can only exist at finite temperature.

The situation is different at finite bias: the rough phase can be induced by finite μ in the quantum limit. This was demonstrated in Ref. [11] in the case of short-range interactions [that is, $\tilde{G}_2 = 0$ in Eq. (16)]. Furthermore, the dislocation compressibility in this case can be described within the Gaussian approach treating the dislocation as an elastic string. Here we address the question of how the bias by μ affects the dislocation in the presence of long-range forces.

The results of simulations of the model in Eqs. (15) and (16) at finite μ and $\tilde{G}_2$ are presented in Fig. 5. It shows that chemical potential induces roughening of the dislocations by restoring the giant compressibility. More specifically, at low values of μ the dislocation is characterized by κ independent of the dislocation length. (This state is marked as "smooth" in Fig. 5). Upon increasing μ the system undergoes the transformation into the rough phase (marked as "rough" in Fig. 5) characterized by the value of $\kappa = \kappa_1$ diverging as $L \to \infty$. The values of G_1, G_2 are chosen so that at $\mu = 0$ the dislocation is in the TLL phase. In this case, while κ, κ_1 show dramatic change, the superfluid stiffness ρ_s remains practically unaffected.

Results of the simulations at $G_{1R} > G_c$, that is, when the dislocation is in the insulating regime at low μ, are shown in Fig. 6. As μ increases, both ρ_s and κ_1 undergo a strong crossover to the non-TLL phase, that is, where there is superfluidity along the core (as well as the ODLRO as explained in Sec. II C).

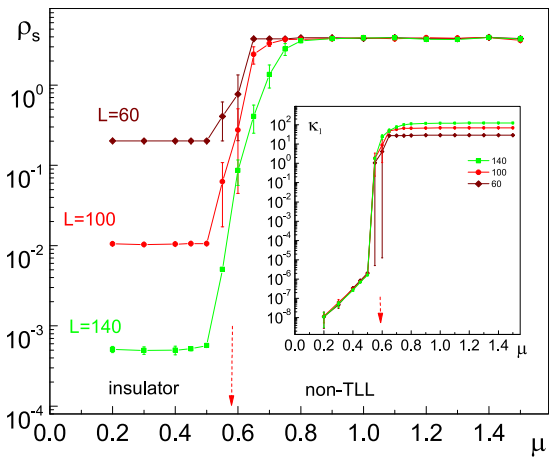

FIG. 6. Superfluid stiffness along the dislocation vs μ undergoing the transformation from the insulating to the non-TLL phase for different lengths L (shown close to each curve); $T = 0.05$. Inset: corresponding κ_1 vs μ.

Compressibility at finite bias in the $T = 0$ limit

Here we focus on the nature of the quantum rough phase of the dislocation and will show that this phase can be described quite accurately within the Gaussian approximation. In other words, an external bias by finite μ can restore superclimb in the quantum limit and in this phase the compact nature of the superfluid phase ϕ can be ignored. As explained in Sec. II C, this phase is non-TLL which has the "paradoxical" ODLRO in 1D.

Here we compare the results of MC simulations of the full quantum action in the limit where κ and κ_1 show saturation at large μ (that is, corresponding to the region $\mu > 0.1$ in the graph Fig. 5) with the Gaussian approximation for κ, Eq. (19), which can be expressed as

$$\kappa = \frac{1}{L}\sum_{x,x'}[\langle Y(x)Y(x')\rangle - \langle Y(x)\rangle\langle Y(x')\rangle], \tag{22}$$

where $Y(x) = (\Delta\tau/\beta)\sum_\tau y(x,\tau)$ corresponds to the Matsubara frequency $\omega = 0$. Similarly, using definition (20) one can represent

$$\kappa_1 = \frac{1}{L\mu}\sum_x \langle Y(x)\rangle. \tag{23}$$

The variable $Y(x)$ corresponds to $\omega = 0$, and it separates from higher Matsubara harmonics ω. This allows us to evaluate the averages $\langle\cdots\rangle$ in Eqs. (22) and (23) within the "shortened" action (12) where only the three last terms are taken into account and only the harmonic $\omega = 0$ is selected. This action then takes the form

$$S_{\rm cl} = \frac{1}{T}\sum_x\left[\frac{G_1}{2}(\nabla_x Y_x)^2 - \mu Y_x + \sum_{x'}\frac{G_2}{2(1+|x-x'|)}\nabla_x Y_x \nabla_{x'} Y_x\right], \tag{24}$$

which is the action for classical string $S_{\rm cl} = E/T$ determined by the potential energy E of elastic deformations. Accordingly, the statistical averaging is to be performed with the classical partition function $Z_{\rm cl} = \int DY\exp(-S_{\rm cl})$.

At this point we note that the long-range term in action (24) is taken in the form which does not satisfy periodic boundary conditions. Therefore, the analytical diagonalization by Fourier transformation becomes impossible. Alternatively, if the distance $|x-x'|$ between two points along the core in Eq. (24) is defined modulo L, such a diagonalization becomes possible. This approach, however, does not correspond to the realistic situation of a dislocation pinned at two points and which is a straight-line string in its equilibrium. Thus, we have resorted to the exact diagonalization of action (24).

Representing

$$Y(x) = \sqrt{\frac{2}{L}}\sum_{n=1}^{L-1}\sin(q_n x) f_n \tag{25}$$

in terms of the spatial harmonics obeying the zero boundary condition, where f_n are real variables with $q_n = \pi n/L$, $n = 1,2,\ldots,L-1$, and substituting it into Eq. (24),

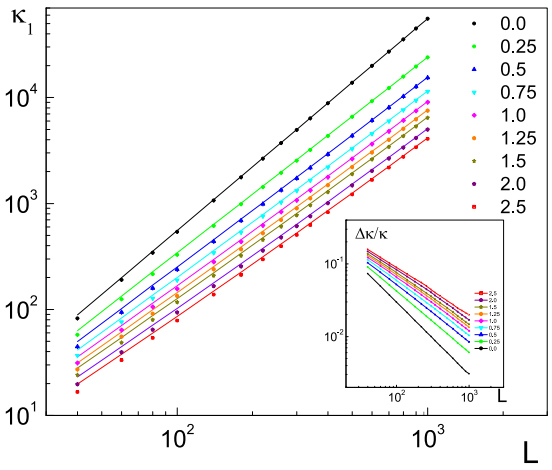

FIG. 7. MC data (points) for κ_1 in the rough state vs the dislocation length L and for various G_2 values (shown in the legend) with $G_1 = 1.5$, $1/T = 20$, and $\rho_0 = 4$. The lines show corresponding results for κ_1, Eq. (20), derived within the Gaussian approximation (30). Inset: the relative deviations between the MC data and the approximation. The decay is characterized by $\sim L^{-c}$ with some exponent ~ 1 [$c = 0.77(2)$ for $G_2 = 1.00$].

we find

$$Z_{\rm cl} = \int Df_n \exp(-S_{\rm cl}), \tag{26}$$

$$S_{\rm cl} = \frac{1}{T}\left[\frac{1}{2}\sum_{n,n'}V_{n,n'}f_n f_{n'} - \mu\sum_n \Phi_n f_n\right], \tag{27}$$

$$\Phi_n \equiv \sqrt{\frac{2}{L}}\frac{[1-(-1)^n]}{2}\cot[\pi n/(2L)], \tag{28}$$

where

$$V_{n,n'} = G_1(Q_n)^2\delta_{n,n'} + \frac{2}{L}\sum_{x,x'}\frac{G_2 Q_n Q_{n'}}{1+|x-x'|} \times \cos[q_n(x+1/2)]\cos[q_{n'}(x'+1/2)], \tag{29}$$

$Q_n \equiv 2\sin(q_n/2)$, and the summations run over $x,x' = 0,1,\ldots,L$.

The averages in Eqs. (22) and (23) can be expressed as

$$\kappa = \kappa_1 = \frac{1}{L}\sum_n\langle\Phi_n f_n\rangle = \frac{1}{L}\sum_{n,n'}\Phi_n(V^{-1})_{n,n'}\Phi_{n'}, \tag{30}$$

where $(V^{-1})_{n,n'}$ is the matrix inverse to $V_{n,n'}$ (which was evaluated by exact diagonalization). These values are the compressibilities obtained within the Gaussian approximation.

The comparison between this approximation (lines) and the MC data (symbols) are shown in Fig. 7. As can be seen, the quality of the Gaussian approximation improves as dislocation length increases. Thus, it is fair to conclude that the quantum rough phase induced by the bias can be well described within the Gaussian approximation, with the deviations reduced below 1% for sizes $L > 200$–300.

VI. DISCUSSION

Here we have focused on the stability of the phase diagram of edge dislocation with a superfluid core with respect to elastic

long-range interactions between jogs. As shown in Ref. [11] for the case of short-range interactions, such a diagram features three quantum phases in the space of three parameters (ρ_0, G_1, μ): (i) TLL which is also the smooth superfluid phase, (ii) the insulator, which is smooth and nonsuperfluid, and (iii) quantum rough, the superclimbing phase induced by finite bias μ. The main result of the present work is demonstrating that the long-range interactions do not change this picture qualitatively. The question is why there is such a significant difference between superclimbing and gliding dislocations, where the long-range interaction eliminates a quantum phase transition [12].

It has been shown in Ref. [12] that the elastic long-range forces suppress the quantum roughening transition for gliding dislocation aligned with Peierls potential. In terms of the dual representation of this dislocation by the Coulomb gas approach this means that the effective interaction between instanton and anti-instanton becomes modified, from log to the log-log of the distance between an instanton pair. This implies that such pairs proliferate at arbitrary small value of the "Coulomb" interaction. Accordingly, the plasma phase of the pairs guarantees that the dislocation is quantum smooth. In other words, an arbitrary weak Coulomb-type interaction eliminates the BKT quantum roughening phase transition for gliding dislocation.

Our current numerical results show that the presence of the superfluid core in edge dislocation changes the situation qualitatively. As a result, the phase diagram of the superclimbing dislocation retains its structure obtained without the "Coulomb" interactions [11]. At a formal level, the difference between two models is easier to understand in terms of the dual representation by the J currents. In the case of the gliding dislocation [12] the duality transformation generates terms with the $\sim 1/r$ interaction between the J currents. In this sense the Coulomb interaction suppresses the Luttinger parameter logarithmically and, thus, eliminates the BKT transition for the gliding dislocation for arbitrary small G_2. In contrast, the edge dislocation with a superfluid core is described by the model in Eqs. (15) and (16) where the Coulomb-type term acts between spatial derivatives of the J currents (oriented along an imaginary time). Thus this interaction vanishes in the long-wave limit and, accordingly, no suppression of the Luttinger parameter occurs, at least, not in the limit $G_2 \to 0$. As was discussed above, the role of the long-range forces is reduced to the renormalization of the parameter G_1.

An unexpected property of the quantum rough phase is the ODLRO in 1D (along the core). This phase can be induced by the bias μ, and its description can be well achieved within the Gaussian model. The exact nature of the transition between TLL (or insulator) and the rough phase is not fully understood. As demonstrated in Ref. [11], the transition is characterized by strong hysteresis at low T. This indicates first-order transition which should occur in the limit $T \to 0$. The question is if the transition remains at finite T. In Ref. [21] the roughening transition has been analyzed for the dislocation aligned with the Peierls potential, and the argument has been given that the transition remains at finite T, in spite of the "no-go" theorem [22] for a phase transition in 1D at finite T. The main argument is that the rough phase is not characterized by any local order parameter with respect to the dislocation shape. Instead, it is a global property of the system. This immediately undermines the basis for the theorem [22]. Thus, the same argument should hold for a generic dislocation so that the first-order roughening transition rather than a crossover occurs at finite T.

ACKNOWLEDGMENTS

This work was supported by the National Science Foundation under Grant No. DMR1720251 and by the China Scholarship Council. We also acknowledge support from the CUNY High Performance Computing Center by providing computational resources.

[1] F. R. N. Nabarro, *Theory of Crystal Dislocations* (Dover, New York, 1987).
[2] B. V. Petukhov and V. L. Pokrovskii, Sov. Phys. JETP **36**, 336 (1973).
[3] V. M. Nabutovski and V. Ya. Shapiro, Sov. Phys. JETP **48**, 480 (1978).
[4] I. N. Khlyustikov and M. S. Khaikin, Sov. Phys. JETP **48**, 583 (1978).
[5] M. Boninsegni, A. B. Kuklov, L. Pollet, N. V. Prokof'ev, B. V. Svistunov, and M. Troyer, Phys. Rev. Lett. **99**, 035301 (2007).
[6] L. Pollet, M. Boninsegni, A. B. Kuklov, N. V. Prokof'ev, B. V. Svistunov, and M. Troyer, Phys. Rev. Lett. **101**, 097202 (2008); **101**, 269901(E) (2008).
[7] M. W. Ray and R. B. Hallock, Phys. Rev. Lett. **100**, 235301 (2008).
[8] Ş. G. Söyler, A. B. Kuklov, L. Pollet, N. V. Prokof'ev, and B. V. Svistunov, Phys. Rev. Lett. **103**, 175301 (2009); **104**, 069901(E) (2010).
[9] M. W. Ray and R. B. Hallock, Phys. Rev. B **81**, 214523 (2010).
[10] A. B. Kuklov, L. Pollet, N. V. Prokof'ev, and B. V. Svistunov, Phys. Rev. B **90**, 184508 (2014).
[11] M. Yarmolinsky and A. B. Kuklov, Phys. Rev. B **96**, 024505 (2017).
[12] D. Aleinikava, E. Dedits, A. B. Kuklov, and D. Schmeltzer, Europhys. Lett. **89**, 46002 (2010).
[13] J. P. Hirth and J. Lothe, *Theory of Dislocations* (McGraw-Hill, New York, 1968).
[14] A. M. Kosevich, *The Crystal Lattice: Phonons, Solitons, Dislocations, Superlattices* (Wiley, New York, 2005).
[15] A. B. Kuklov, Phys. Rev. B **92**, 134504 (2015).
[16] J. Villain, J. Phys. (Paris) **36**, 581 (1975); W. Janke and H. Kleinert, Nucl. Phys. B **270**, 135 (1986).
[17] M. Wallin, E. S. Sørensen, S. M. Girvin, and A. P. Young, Phys. Rev. B **49**, 12115 (1994).
[18] E. L. Pollock and D. M. Ceperley, Phys. Rev. B **36**, 8343 (1987).
[19] N. V. Prokof'ev, B. V. Svistunov, and I. S. Tupitsyn, Phys. Lett. A **238**, 253 (1998); JETP **87**, 310 (1998).
[20] B. V. Svistunov (private communication).
[21] D. Aleinikava and A. B. Kuklov, Phys. Rev. Lett. **106**, 235302 (2011).
[22] L. D. Landau and E. M. Lifshitz, *Statistical Physics, Part 1: Vol. 5. Course of Theoretical Physics*, 3rd ed. (Butterworth-Heinemann, Oxford, 2000), p. 537.